HHS Public Access

Author manuscript

Stem Cell Res. Author manuscript; available in PMC 2021 June 30.

Published in final edited form as:

Stem Cell Res. 2021 May ; 53: 102318. doi:10.1016/j.scr.2021.102318.

Endothelial cell secreted VEGF-C enhances NSC VEGFR3 expression and promotes NSC survival

Rita Matta[a], **Yan Feng**[b,c], **Lauren H. Sansing**[b,*], **Anjelica L. Gonzalez**[a,*]

[a]Department of Biomedical Engineering, Yale University, New Haven, CT 06511, USA

[b]Department of Neurology, Yale University School of Medicine, New Haven, CT 06511, USA

[c]Department of Neurology, Tianjin Medical University General Hospital, Tianjin, China

Abstract

Although delivery of neural stem cell (NSC) as a therapeutic treatment for intracerebral hemorrhage (ICH) provides promise, NSC delivery typically has extremely low survival rates. Here, we investigate endothelial cell (EC) and pericyte (PC) interactions with NSC, where our results demonstrate that EC, and not PC, promote NSC cell proliferation and reduce cytotoxicity under glucose deprivation (GD). Additionally, NSC proliferation was increased upon treatment with EC conditioned media, inhibited with antagonism of VEGFR3. In an NSC + EC coculture we detected elevated levels of VEGF-C, not seen for NSC cultured alone. Exogenous VEGF-C induced NSC upregulation of VEGFR3, promoted proliferation, and reduced cytotoxicity. Finally, we delivered microbeads containing NSC + EC into a murine ICH cavity, where VEGF-C was increasingly present in the injury site, not seen upon delivery NSC encapsulated alone. These studies demonstrate that EC-secreted VEGF-C may promote NSC survival during injury, enhancing the potential for cell delivery therapies for stroke.

Keywords

VEGF-C; VEGFR3; Neural stem cell; Stroke

1. Introduction

Intracerebral hemorrhagic stroke (ICH) is directly associated with a mortality rate of approximately 40–60% one year post event (Flaherty et al., 2006; Sacco et al., 2009). Despite the high rate in death following ICH, there has been relatively little research focused

*Corresponding authors. lauren.sansing@yale.edu (L.H. Sansing), anjelica.gonzalez@yale.edu (A.L. Gonzalez).

Author contributions

R.M. and A.L.G. conceived the experiments, conducted *in* vitro experiments, created microbeads with or without encapsulated cells, and wrote the manuscript. Y.F and L.H.S. conceived the experiments, conducted *in vivo* work, and wrote the manuscript.

Declaration of Competing Interest

The authors declare that they have no known competing financial interests or personal relationships that could have appeared to influence the work reported in this paper.

Appendix A. Supplementary data

Supplementary data to this article can be found online at https://doi.org/10.1016/j.scr.2021.102318.

on the mechanisms of injury and repair, as compared to research conducted on ischemia. ICH survivors are afflicted with broad neurological tissue impairments, making ICH the least treatable form of stroke (Chiu et al., 2010). The immediate introduction of blood components, including leukocytes, erythrocytes, platelets, and proteins such as thrombin and fibrinogen, into the intracerebral space, and subsequent tissue injury induces a neuro-inflammatory response. Neuroinflammation is directly responsible for the subsequent increase in astrocyte abundance in the damaged area, contributing to formation of the glial scar (Sukumari-Ramesh et al., 2012). There is potential, however, to harness the endogenous mechanisms that promote the reparative process, to facilitate effective therapeutics that limit neurological damage and facilitate regenerative repair following ICH.

Stem cell therapies have the potential to replace dead and dying cells following acute stroke and restore damaged neural circuitry and inhibit degenerative responses to tissue injury cues caused by stroke. Therapeutic intervention can use stem cell delivery as an approach to introduce healthy and viable cells to the damaged surrounding tissue in the hemorrhaged area. Neural stem cells (NSC) in particular hold promise due to their ability to differentiate into functionally specific cells following injury cues (Lindvall and Kokaia, 2010). Despite the potential benefits, NSC delivery to the injured brain remains restricted in clinical translation due to low rates of cell survival post transplantation (Hicks et al., 2009). Tissue engineering strategies could lend solutions to both cell injury during delivery and cell survival following implantation.

In healthy brain tissue, NSC within the germinal regions of the adult brain interact closely with the vasculature and its cellular components, including endothelial cells (EC) and pericytes (PC). The vasculature is critical for providing intrinsic signals and extrinsic cues to the NSC within the neurogenic niches (Ottone and Parrinello, 2015). Specifically, NSC contact the vasculature directly in the germinal subventricular zone (SVZ), the largest area in the adult brain where neurogenesis occurs (Alvarez-Buylla and García-Verdugo, 2002). Beyond direct functional signaling of the NSC, vascular proliferation and neurogenesis are regulated by many of the same factors. Both neurogenesis and angiogenesis are enhanced during injury, and there is upregulation of neurotrophic factors such as brain-derived neurotrophic factor (BDNF) and angiogenic factors like vascular endothelial growth factor (VEGF) (Jin et al., 2002; Zhang et al., 2014a, 2014b). Interestingly, VEGF-C, the main lymphangiogenic factor, activates NSC without inducing vascular proliferation, unlike VEGF-A. This difference in VEGF signaling suggests that VEGF-C is an activator of NSC in the SVZ and a regulator of neurogenesis in developing and adult brains (Le Bras et al., 2006; Calvo et al., 2011). VEGFR3, the high affinity receptor of VEGF-C, is expressed in NSC. The conditional deletion of VEGFR3 led to a reduction in the number of dividing neural cells (Calvo et al., 2011; Han et al., 2015). VEGF-C secretion and VEGFR3 expression is induced in reactive astrocytes, infiltrated macrophages, and activated microglia in a rat ischemic model (Shin et al., 2015), however the role of EC and PC secreted VEGF-C on NSC survival has yet to be elucidated.

Here, our objective is to probe the role of vascular secreted VEGF-C in promoting NSC survival during injury through NSC VEGFR3 signaling, which remains unknown. We use a glucose deprivation model (GD), as opposed to an oxygen-glucose deprivation model

(OGD), since glucose has been demonstrated to be the survival limiting factor within the classic OGD (Singh et al., 2009). Our results demonstrate that EC, though not PC, promote NSC proliferation and reduce cytotoxicity during GD. We also show that NSC proliferation is partially restored following GD when NSC are treated with EC conditioned media containing EC secreted VEGF-C. Beyond the role of EC secreted VEGF-C, we find that exogenous VEGF-C reduces NSC cytotoxicity, enhances proliferation, and increases VEGFR3 expression following GD, suggesting a pro-survival role of VEGF-C/VEGFR3. To demonstrate application of our in vitro results, we deliver degradable polyethylene glycol (PEG) microbeads containing co-encapsulated NSC and EC into the hemorrhagic stroke brain. The delivery of co-encapsulated NSC and EC within polymeric microbeads leads to increased VEGF-C secretion, not seen for NSC delivered alone. Together, the results of these studies suggest a beneficial therapeutic effect of VEGF-C/VEGFR3 signaling in response to injury by enhancing NSC survival.

2. Methods

2.1. Cell maintenance

Adherent neural cell line (ANS4) have been characterized by S. Pollard (Pollard et al., 2006) to be cultured in serum-free conditions. For tracking *in vivo* and in vitro co-cultures, GFP transfected ANS4s were utilized (NSC-GFP) (Bressan et al., 2017). The commercially available immortalized mouse brain endothelial cell line (bEND.3, ATCC) and mouse brain vascular pericytes cell line (MBVP, ScienCell) were cultured according to manufacturer's protocol. To deprive cells of glucose, a confluent cell layer was gently washed 3 times in 1X PBS and replaced with glucose-free NBM-27 media (Invitrogen) and were maintained at 37 °C in 5% CO_2 atmosphere for 4 or 24 h.

2.2. Cell proliferation and cell cytotoxicity assay

Cell proliferation and cell cytotoxicity were measured using MTT (ThermoFisher) and LDH (ThermoFisher) assays, respectively, following the manufacturer's protocols. NSC, NSC + EC, and NSC + PC were cultured in a 96 well plate at a cell-density of 10,000 cells/well. For co-cultures, a 1:1 ratio was used and maintained in NSC media. Monolayers were gently washed following 24 h of culture, and media was replaced with GD media for 4 and 24 h. An MTT stock was prepared at a concentration of 5 mg/ml in PBS and added to each well at a concentration of 0.005 mg/ml. Samples were incubated for 2 h and absorbance was read at 570 nm.

The LDH assay was conducted following the culture of cells as mentioned above for baseline and glucose deprived samples, extra wells were cultured for spontaneous LDH and maximum LDH assessment. After 4 and 24 h of glucose deprivation, the assay was conducted. Sterile ultrapure water and lysis buffers were added to designated wells for spontaneous and maximum LDH controls, respectively, and incubated for 45 min. Next, samples were transferred to a 96-well plate with added reaction mixture and incubated for 30 min. After addition of the stop solution, absorbance was measured at 490 and 680 nm.

2.3. Conditioned media treatment

NSC, EC, PC, and EC + PC were cultured in a 12 well plate at a seeding density of 100,000 cells/ml in NSC media. After 24 h in culture, conditioned media (CM) was collected from EC, PC, and EC + PC, and the NSC monolayers were gently washed 3 times with 1X PBS. CM was gently added to the NSC monolayers which were then imaged at 4 and 24 h.

2.4. VEGF-C and VEGFR3 detection

VEGF-C secretion in culture media was detected using a VEGF-C ELISA (NovusBio) following the manufacturer's protocol. In brief, NSC, NSC + EC, and EC media were plated at a density of 100,000 cells/ml in 12 well plates in NSC media under baseline or GD. Media was collected at 4 and 24 h for both conditions. Following protocol, absorbance was immediately measured at 450 nm.

For immunostaining of VEGF-C and VEGFR3, NSC, NSC + EC, and EC were cultured on laminin coated coverslips for 24 h. Next, cells either remained at baseline or were glucose deprived for 4 h. The cells were fixed with 4% PFA, blocked and permeabilized, and stained overnight with rat anti-VEGFR3 (Invitrogen, 1:100) or rabbit anti-VEGF-C (NovusBio, 1:100), and phalloidin. The following day, respective secondary antibodies were added, and cells were imaged using fluorescent microscopy (Leica). VEGFR3 expression was also quantified using flow cytometry. Following 4 and 24 h of GD, NSC, NSC from NSC + EC, and EC were collected, where NSC in co-culture were detached using Accutase, ensuring EC remained adherent to the culture well. The cells were fixed with 4% PFA, blocked and permeabilized, and stained overnight. The following day, after secondary incubation, flow cytometry was conducted against VEGFR3 (NovusBio, 1:100 and analysis was done using FlowJo.

2.5. VEGFR3 antagonism

SAR131675 (Selleckchem) is a VEGFR3 inhibitor with IC50/K_i of 23 nM/12 nM in cell-free assays, about 50- and 10-fold more selective for VEGFR3 than VEGFR1/2 and has little activity against Akt1, CDKs, PLK1, EGFR, IGF-1R, c-Met, and Flt2 (Blanc et al., 2010; Alam et al., 2012; Espagnolle et al., 2014). SAR131675 was diluted to a 5 mM concentration in DMSO and following incubations at baseline or glucose deprivation, NSC VEGFR3 was blocked at a concentration of 50 nM for 24 h.

2.6. Exogenous VEGF-C treatment

Recombinant VEGF-C (Sigma) was reconstituted in 0.1% acetic acid to a concentration of 0.1 mg/ml. NSC were plated at a density of 100,000 cells/ml in 12 well plates in NSC media. Following 24 h of culture, culture media was changed to GD media. After 4 h of GD, VEGF-C was added at a concentration of 10 ng/ml. For comparison, NSC were also maintained at baseline or maintained under GD for an additional 24 h. All conditions were then assessed using an MTT and LDH assay as described above. In addition, NSC were collected and VEGFR3 was quantified via flow cytometry as described above.

2.7. Synthesis of PEGDA and PEG derivatives

Polyethylene glycol diacrylate (PEGDA) was prepared as previously described (Gonzalez et al., 2004; Lauridsen et al., 2014; Matta et al., 2019). In order to create bioactive PEG derivatives, adhesive peptides and an MMP degradable sequence were conjugated to PEG using previously described methods (Matta et al., 2019; Ghuman et al., 2020). The fibronectin derived peptide arginine–glycine–aspartic acid-serine (RGDS) and laminin derived peptide tyrosine-isoleucine-glycine-serine-arginine (YIGSR) have each demonstrated the ability to support cell adhesion of EC and NSC, respectively (Gonzalez et al., 2004; Lampe and Heilshorn, 2012). RGDS and YIGSR were reacted with acryloyl-PEG-N-hydroxysuccinimide Ester (PEG-NHS, 3500 Da) in 50 mM sodium bicarbonate (pH 8.5) at a 1:1 (peptide: PEG) molar ratio for 2 h at room temperature, dialyzed, frozen, and lyophilized. Degradable constructs were created through the conjugation of the degradable sequence glycine-glycine-leucine-glycine-proline-alanine-glycine-glycine-lysine (GGLGPAGGK; LGPA) to PEG as previously described (Lee et al., 2007; Matta et al., 2019), reacting LGPA in sodium bicarbonate at a 1:2 (peptide:PEG) molar ratio for 24 h at room temperature. The polymer was then dialyzed, frozen, and lyophilized. Lastly, for tracking of microbeads *in vivo*, a fluorescent tag was conjugated by dissolving PEG-RGDS in 0.1 M sodium bicarbonate buffer (pH 8.5) and dissolving Alexa Fluor™ 488 (AF-488) NHS Ester (Succinimidyl Ester) (ThermoFisher Scientific) in dimethylsylfoxide (DMSO, 1 mg/100 μl). AF-488 was added to PEG-RGDS at a 10:1 M ratio of dye to conjugated polymer, reacted for 2 h at room temperature, then dialyzed for 24 h, frozen, and lyophilized.

2.8. Microbead synthesis

Recently, we created and optimized PEG microbeads, either degradable or non-degradable, with or without encapsulated cells (Matta et al., 2019; Ghuman et al., 2020). In brief, we use an oil emulsion technique where we combine 25 μl of aqueous pre-gel solution containing 0.1 g/mL 10 kDa PEGDA, 1.5% (v/v) triethanolamine in 1X Dulbecco's Phosphate Buffered Saline (PBS), 3.4 μl/mL 1-Vinyl-2-pyrrolidinone, 10 μM Eosin Y, and 0.25% (v/v) Pluronic to an oil phase, containing 3 μl photoinitiator (300 μg 2, 2-dimethoxy-2-phenyl-acetophenone/ ml NVP) per ml mineral oil. The phases were then vortexed for 13 s and exposed to white light for 3 min. Microbeads were separated from the oil phase through a series PBS washes, centrifuging for 5 min at 1200 RPM, decanting mineral oil between washes. To add a fluorescent tag to microbeads, 2 mM PEG-RGDS-AF488 was added to the pre-gel solution. For cell encapsulated microbeads, 2 mM PEG-YIGSR and 2 mM PEG-RGDS were added to the aqueous pre-gel solution (Matta et al., 2019; Ghuman et al., 2020). NSC and EC pellets were resuspended in pre-gel at a final concentration of 75×10^6 cells/ml, using NSC:EC at a 1:1 ratio. Next, 25 μl of the pre-gel and cell suspension were mixed thoroughly and added to the mineral oil phase as previously mentioned. The polymer and cell phase were crosslinked with white light, then separated from the oil phase through washes with NSC media and decanting the oil phase. Lastly, microbeads were transferred to a well plate and maintained in the incubator for 48 h prior to ICH brain injections.

2.9. Animals

C57BL/6 mice were purchased from Jackson Laboratories. All mice were bred under specific-pathogen-free conditions with a 12-hour light/dark cycle in a temperature-controlled environment and ad libitum access to water and food pellets. All experimental protocols were conducted in accordance with the NIH guidelines and were approved by the Yale Institutional Animal Care and Use Committee.

2.10. Collagenase ICH mouse model and microbeads injection

The mice were anesthetized through 2–5% isoflurane inhalation and ventilated with oxygen-enriched air (20:80%). To create an ICH lesion, mice were injected with 1 μl of 0.24 U type VII collagenase (from Clostridium histolyticum, Sigma-Aldrich) at a rate of 0.2 μl/min into the right striatum relative to the bregma: 2.1 mm lateral and 3.5 mm deep. The craniotomy was sealed with bone wax, and the scalp was closed with tissue adhesive (3 M Vetbond). During the surgery, rectal temperature was maintained at 37.0 ± 0.5 °C throughout the experimental and recovery periods (DC Temperature Controller 40–90-8D; FHC Inc.).

After 7, 14, or 28 days of ICH collagenase injection, mice were anesthetized by isoflurane as mentioned above. Microbeads were injected at the same injection point, depth and speed as mentioned above. Prior to sacrificing mice at 24 or 48 h after microbead injection, Brefeldin-A was injected through a tail vein injection for each mouse using previously described methods (Foster et al., 2007). In brief, a 0.25 mg/ml solution of Brefeldin-A was made, and 100 μl was injected to the tail vein of each mouse using an insulin syringe 6 h prior to sacrifice.

2.11. Tissue processing and immunohistochemistry

Mice were transcardially perfused with 20 ml PBS followed by 20 ml 4% PFA. Brains were then harvested and post-fixed in 4% PFA overnight at 4 °C. Next, brains were transferred to 30% sucrose for 48 h and embedded in OCT. Sections were cut at a thickness of 50 μm and stored in 30% glycerin prior to imaging.

Sections were rinsed 3 times in PBS and blocked and permeabilized with 5% normal donkey serum and 2% Triton X-100 in PBS for 1 h at room temperature. Sections were then incubated with the following antibodies at 4 °C overnight: chicken anti-GFP (Abcam, 1:1000), rabbit Iba-1 (NovusBio, 1:100), and rabbit anti-VEGF-C (NovusBio, 1:100). The following day, respective secondary antibodies were added for 2 h at room temperature, sections were mounted using Dapi mounting media, and images were taken using a fluorescent microscope (Leica).

2.12. Statistics

All statistical analyses were performed using GraphPad Prism software. Significance was determined with either a one-way ANOVA with multiple comparisons, or by an unpaired *t*-test as appropriate. Data were expressed as mean ± SEM and the differences were considered significant at P values of < 0.05.

3. Results

3.1. EC increase NSC proliferation and decrease NSC cytotoxicity during glucose deprivation

EC are known to promote NSC survival, proliferation, and differentiation post transplantation into the ischemic injured brain (Nakagomi et al., 2009). Although this pro-survival effect of EC on NSC has been demonstrated in oxygen-glucose deprivation models, it has not been investigated solely in the absence of glucose (Xiong et al., 2013). To investigate the role of EC and PC in promoting NSC survival during GD, we cultured NSC, NSC + EC, and NSC + PC in a 1:1 ratio, and then deprived samples of glucose for 4 or 24 h. NSC cultured alone appear unhealthy and unattached by 24 h, mostly floating or dead (Fig. 1A), however NSC-GFP in the presence of EC remain adherent to the culture well, in a clustered phenotype (Fig. 1A). On the other hand, NSC-GFP in the presence of PC look unhealthy, unattached, and fragmented by 24 h (Fig. 1A). We quantified cell proliferation at 4 and 24 h using an MTT assay (Fig. 1B), which assesses cell metabolic activity and reflects the number of viable cells present. After 4 and 24 h, NSC had a significant reduction in proliferation ($P < 0.0001$) compared to NSC baseline control. Interestingly, there was no significant difference between NSC + EC after 4 and 24 h of glucose deprivation compared to NSC baseline control ($P = 0.8588$ and $P = 0.1740$, respectively). In addition, there is a significant decrease in proliferation for NSC under glucose deprivation versus NSC + EC under glucose deprivation at 4 and 24 h ($P = 0.0001$ and $P < 0.0001$, respectively), suggesting EC promote NSC survival. In contrast, we see a significant reduction in NSC proliferation for NSC + PC at 4 and 24 h ($P < 0.0001$ and $P = 0.0001$, respectively). These results were supported by the results of an LDH assay, measuring extracellular lactate dehydrogenase, to assess cytotoxicity (Fig. 1C). NSC under 4 and 24 h of GD had a significant increase in cytotoxicity, as compared to NSC baseline control ($P < 0.0001$). On the other hand, we see no significant difference in cytotoxicity at 4 and 24 h for NSC + EC compared to NSC baseline control ($P = 0.9067$ and $P = 0.0655$, respectively). There is a significant increase in cytotoxicity for NSC under glucose deprivation versus NSC + EC under glucose deprivation at 4 and 24 h ($P = 0.0009$ and $P = 0.0013$, respectively), suggesting EC reduce cytotoxicity. In contrast, NSC cultured with PC, exhibited a significant increase in cytotoxicity at both time points, as compared to NSC baseline control ($P = 0.0007$ and $P = 0.0009$, respectively). We also cultured EC and PC up to 48 h under GD and evaluated their cytotoxicity to ensure effects seen were due to NSC, and not EC or PC (Figure S1). In total, the results suggest that EC, and not PC, are contributors to NSC proliferation and reduced NSC cytotoxicity in response to glucose deprivation.

3.2. VEGF-C secretion is increased in co-cultures of NSC + EC during glucose deprivation

VEGFR3 is present in SVZ resident NSC and VEGF-C is synthesized in the lateral ventricle walls, suggesting that VEGF-C may stimulate NSC expressing VEGFR3. In addition, overexpression of VEGF-C has led to stimulation of NSC VEGFR3, positively impacting neurogenesis in the SVZ (Calvo et al., 2011). To investigate the role of EC secreted VEGF-C, we quantified VEGF-C secretion through an ELISA at 4 and 24 h for NSC, NSC + EC, and EC at baseline and GD (Fig. 2A–B). For NSC, there was a slight increase in VEGF-C

secretion during GD compared to baseline at 4 h ($P = 0.0027$), and there is no significant change in VEGF-C secretion at 24 h ($P = 0.1330$). In contrast, NSC + EC had a significant increase in VEGF-C expression during GD compared to baseline at both 4 and 24 h ($P < 0.0001$ and P = 0.0002, respectively). EC alone had similar VEGF-C secretion during baseline and GD at 4 h ($P = 0.7898$) and an increase at 24 h ($P = 0.0010$). Since EC VEGF-C levels are about two-fold higher compared to NSC under GD at 4 and 24 h, and this increase is similar for NSC + EC, these data suggest EC are the main secretors of VEGF-C during GD.

We conducted immunofluorescent staining to visualize VEGF-C nuclear and cytoplasmic localization during baseline and GD at 4 h (Fig. 2C–D). NSC have nuclear staining for VEGF-C during both conditions, seen through co-localization of VEGF-C and Dapi. For a co-culture of NSC + EC, we distinguish the two cell types by their nuclear size stained with Dapi and cell cytoskeleton stained with Phalloidin; NSC, have small nuclei with thin, long bodies, and EC have much larger nuclei with large, extended bodies. For reference, an example of a typical NSC or EC have been distinguished by arrows (yellow and white, respectively). In co-culture, EC have both nuclear and cytoplasmic presence of VEGF-C, and this is seen more intensely during GD. This agrees with our ELISA data, suggesting EC secrete higher levels of VEGF-C during GD when co-cultured with NSC. We see a similar pattern for EC nuclear and cytoplasmic staining for monocultures of EC under GD, further supporting our hypothesis that EC secreted VEGF-C both under resting conditions and further increased may act upon NSC during GD.

3.3. NSC VEGFR3 expression is increased in Co-Cultures of NSC + EC

VEGF-C stimulates neurogenesis by directly interacting with VEGFR3 on neural cells (Han et al., 2015). In addition, deletion of VEGFR3 within NSC negatively impacts neurogenesis in the mouse SVZ (Calvo et al., 2011). VEGFR3 is expressed by SVZ NSC, and VEGF-C can stimulate mitosis of VEGFR3 expressing SVZ-derived NSC. In fact, SVZ neurogenesis is VEGFR3 dependent (Calvo et al., 2011). We quantified cell VEGFR3 expression by flow cytometry on NSC, NSC from an NSC + EC co-culture, and EC, during baseline and GD at 4 and 24 h (Fig 3A–B, Figure S2). Interestingly, we see a significant decrease in VEGFR3 expression for mono- cultured NSC following 4 h of GD compared to baseline ($P < 0.0001$), which was no longer significant at 24 h ($P = 0.0537$). This was not the case of NSC cultured with EC, where NSC have a significant increase in VEGFR3 expression at both 4- and 24-hours GD compared to baseline ($P = 0.0106$ and $P < 0.0001$, respectively), suggesting that NSC VEGFR3 expression increases with prolonged GD exposure. EC, on the other hand, expressed VEGFR3 at high levels during baseline, as expected since VEGFR3 is abundant on angiogenic blood vessels (Zarkada et al., 2015). EC VEGFR3 expression remained unchanged following 4 h of GD, and there was an increase following 24 h of GD compared to baseline ($P = 0.0038$). In total, our results suggest that NSC VEGFR3 expression is increased in co-culture with EC, potentially by EC-derived VEGF-C, as shown in Fig. 2.

We conducted immunofluorescent staining to visualize VEGFR3 expression at baseline and 4 h of GD (Fig. 3C). As above, we differentiate NSC from EC in co-cultures by the presence of thin, elongated NSC bodies with small nuclei (indicated with a yellow arrow), as

compared to the large, extended EC bodies with much larger nuclei (indicated with a white arrow). We can visualize the reduction in NSC VEGFR3 expression following 4 h of GD compared to baseline control (Fig 3D), which was unlike NSC VEGFR3 expression when in co-culture with EC. Our immunofluorescent staining complements our flow cytometry data, confirming the changes in NSC VEGFR3 expression during GD.

3.4. EC conditioned media increases NSC proliferation following glucose deprivation when VEGFR3 is not blocked

We have demonstrated that co-culturing with EC, and not PC, has a pro-survival effect on NSC following GD, and identified VEGF-C as a potential mediator of survival and proliferation. We then investigated directly tested whether soluble factors from EC or PC could rescue NSC after GD and support NSC proliferation. We deprived NSC of glucose for 4 h (Fig. 4A), then recovered NSC in cultured media (CM) from EC, PC, and EC + PC for 24 h. We see that NSC recovered in EC CM are adherent, and some cells had a clustered phenotype, which was in stark contrast to NSC recovered in PC CM, which appear to be unhealthy and unattached to the culture well (Fig. 4B). NSC recovered in EC + PC CM appear to be partially adherent, and partially unattached (Fig. 4B).

Next, we tested if NSC can no longer respond to pro-survival cues from supporting cells in the presence of a VEGFR3 antagonist, SAR131675, at a concentration of 50 nM for 24 h. Interestingly, NSC were unhealthy and unattached when recovered in EC CM + VEGFR3 antagonist (Fig. 4C). This was also apparent for NSC with VEGFR3 antagonists recovered in EC + PC CM (Fig. 4C). We then quantified proliferation in this rescue paradigm for the different CM conditions by MTT assay. We found a significant increase in NSC proliferation for NSC recovered in EC CM as compared to NSC remained under GD ($P = < 0.0001$), which was less significant for NSC recovered in PC CM ($P = 0.0220$) (Fig. 4D). When recovered in EC + PC CM, NSC had a significant increase in proliferation compared to NSC remained under GD ($P = < 0.0001$) (Fig. 4D), suggesting EC are the main contributors of soluble factors that have a pro-survival impact on NSC. However, in the presence of the VEGFR3 antagonist, there was no significant difference for recovery in EC CM, PC CM, and EC + PC CM when compared to NSC remaining under GD (Fig. 4D). This suggests that VEGFR3 is crucial for NSC to respond to pro-survival secreted factors, and without VEGFR3, NSC proliferation cannot be restored by EC-secreted factors.

3.5. Exogenous VEGF-C treatment promotes NSC proliferation, decreases cytotoxicity, and increases VEGFR3 expression during glucose deprivation

Having observed that EC secrete VEGF-C, and VEGF-C was significantly higher for NSC + EC under GD compared to baseline, we sought to determine if exogenous VEGF-C promotes NSC health during GD independently of EC. We glucose-deprived a monolayer of NSC for 4 h, then treated the NSC with exogenous VEGF-C at a concentration of 10 ng/ml, maintained for 24 h, or kept the NSC under GD up to 24 h. A NSC monolayer with glucose served as our control. NSC under GD treated with VEGF-C remained mostly adherent, especially compared to NSC under GD with no treatment, which were fragmented and unattached (Fig. 5A). Interestingly, NSC under GD with no treatment had a significant reduction in VEGFR3 expression (less than ½ -fold compared to NSC control) (Fig. 5B). On

the contrary, NSC under GD with VEGF-C treatment have a significant increase in VEGFR3 expression compared to NSC control (~1.5-fold), agreeing with our previous results that VEGFR3 expression is increased with EC co-culture and the increased EC secretion of VEGF-C after GD (Figs. 2 and 3). In addition, we conducted a MTT and LDH assay for cell proliferation and cytotoxicity, respectively. We see a sharp drop in NSC proliferation for NSC remained under GD compared to NSC control (Fig. 5C). In contrast, NSC under GD with VEGF-C treatment had a significant increase in proliferation compared to NSC remained under GD ($P < 0.0001$) (Fig. 5C). Although the addition of VEGF-C does not completely return proliferation to levels of NSC control, our results demonstrate that VEGF-C plays an important role in promoting NSC health following GD. Likewise, our cytotoxicity data demonstrates a significant increase in NSC cytotoxicity under GD compared to control ($P < 0.0001$) and compared to NSC under GD treated with VEGF-C ($P < 0.0001$) (Fig. 5D). Although not completely abrogating cell death, there was a slight increase in NSC cytotoxicity for NSC under GD treated with VEGF-C ($P = 0.0229$) as compared to control (Fig. 5D).

3.6. NSC + EC encapsulated microbeads lead to greater VEGF-C expression in tissue compared to blank microbeads and NSC encapsulated microbeads

Microbeads were created through an dual oil emulsion technique (Figure S3), where microbeads have an average diameter of ~ 150 μm and have undergone optimization for microbead size, cells/microbead, and the cell ratio of NSC + EC co-encapsulated microbeads (Matta et al., 2019). The microbeads are degraded by matrix metalloproteinases, allowing release of cells under inflammatory conditions. Recently, we have demonstrated that NSC co-encapsulated with EC in polymeric PEG microbeads enhanced NSC viability and maintained NSC quiescence compared to NSC encapsulated alone prior to and post injection into a non-injury mouse model. In addition, co-encapsulated NSC + EC microbeads retained NSC survival and quiescence post-delivery to a non-injury mouse model better than NSC encapsulated alone. In addition, the microbeads used to deliver cells did not induce an immune response, compared to freely injected cells, ultimately enhancing cell viability (Matta et al., 2019).

To further assess the delivery of NSC and NSC + EC in microbeads, we began to deliver cell encapsulated microbeads *in vivo* after intracerebral hemorrhage (ICH) (Taylor et al., 2017). After ICH, the brain injury cavity where ideally NSC could help restore function no longer has a blood supply. The resulting nutrient deprivation for cells may impede NSC survival. First, we began optimizing the injection time points by delivering non-degradable, fluorescent microbeads with no encapsulated cells to ensure we were injecting into hemorrhage cavity. We found that 30 days post ICH formation, the cavity was no longer visible (Figure S4), where the microbead injection causes a cavity through the pressure exerted, making this time point unsuitable injections. At 14 days, there is a cavity we can target effectively, however microbeads did not degrade, thus we moved to an earlier time point to capitalize on inflammation leading to microbead degradation. Finally, we concluded that injecting into the cavity 7 days post ICH induction and sacrificing mice 2 days following injection allowed for complete degradation of microbeads as well as cell escape

from the microbeads, in addition to migration along white matter tracts where the hemorrhage commonly extends (Figure S5).

Mice were injected with Brefeldin-A prior to sacrificing animals for processing to maintain cellular localization of secreted factors for immunofluorescent assessment. Brain sections were stained for VEGF-C to assess VEGF-C production by endogenous and exogenous cells in the hemorrhage cavity as well as the tissue surrounding the injury, where the hemorrhage area and injection site is indicated by a white arrow. Degradable microbead constructs with no cells result in little to no VEGF-C secretion surrounding the microbeads or hemorrhage cavity (Fig 6A), as expected, since PEG is known to be an inert material. When NSC were injected alone, there was slight VEGF-C secretion around the injection area (Fig. 6B), where most NSC-GFP$^+$ cells do not express VEGF-C. In addition, there was faint secretion for VEGF-C in the injection area or in the surrounding damaged tissue. However, NSC + EC co-encapsulated microbeads produce high VEGF-C secretion in cells surrounding the microbead constructs, as well as along the injection tract (Fig. 6B). Here, we see many VEGF-C$^+$ cells, unlike when NSC are encapsulated alone, and cells in the injection area as well as throughout the damaged tissue are VEGF-C$^+$. This suggests that both in vitro and *in vivo*, NSC + EC together provide a VEGF-C rich environment in response to injury.

4. Discussion

Stroke is among the leading causes of death and disability worldwide, partly due to the lack of effective therapies that facilitate the recovery of damaged brain tissue (Mozaffarian et al., 2016). In particular, ICH leads to an extremely high mortality rate and inflammatory responses may persist for weeks, leading to an inhabitable environment for NSC (Taylor and Sansing, 2013; Askenase and Sansing, 2016). Stem cell therapies used to treat neurological diseases are promising, owing to their innate ability to enhance endogenous repair mechanisms and promote functional recovery. Stem cell therapy has been investigated for the treatment of ICH and has shown promising results (Gao et al., 2018). However, there are extremely low levels of transplanted cell survival within the inflamed, cytotoxic brain (Smith et al., 2012).

A successful cell delivery strategy can build upon the interactions between NSC and vascular cells to enhance NSC survival *in vivo*, recovering the abundance and differentiation of neurons in the damaged tissue. During injury, NSC from the SVZ, containing the largest pool of proliferating NSC in the adult brain, become activated. NSC directly interact with EC and PC, and studies highlight the interaction between NSC and the vasculature (Nakagomi et al., 2009; Ruan et al., 2015; Azevedo et al., 2017). The molecular mechanisms by which EC and PC impact NSC at homeostasis and during stroke are incompletely described (Park et al., 2002; Lin et al., 2015; Marlier et al., 2015). Diffusible secreted signals from vasculature, specifically EC, are known to increase survival, proliferation, differentiation, and migration of NSC in vitro using an OGD model and *in vivo* during ischemia (Carmichael 2006, Girouard and Iadecola 2006). Here, we investigate the role that VEGF-C plays in NSC survival during GD, which has been speculated to be responsible for NSC transitioning into neuroblasts (Calvo et al., 2011; Han et al., 2015).

We demonstrate that NSC cell contact with EC, but not PC, significantly enhanced NSC proliferation and reduced NSC cytotoxicity during GD. Through our CM studies, we conclude EC CM can significantly enhance NSC proliferation in response to GD as compared to NSC under GD. For NSC with a VEGFR3 antagonist, this proliferation enhancement was diminished, heightening the necessity for VEGFR3. Interestingly, we see that co-cultures of NSC + EC under GD have significantly higher levels of VEGF-C than NSC under GD, where EC alone have the highest secreted levels, suggesting EC are the main contributors to VEGF-C secretion during GD. Along with elevated VEGF-C in co-cultures, we see NSC from NSC + EC co-cultures have significantly higher levels of VEGFR3 during GD, suggesting the correlation of elevated VEGF-C with increased VEGFR3 expression because of the chemokine's availability. These data demonstrate the positive effect of VEGF-C/VEGFR3 during GD and encourage the usage of this cytokine for therapeutic exploration.

Due to NSC dependence on vascular cells for appropriate response during health and disease, a co-transplantation of NSC with a native SVZ cell type may be key to overcoming limitations of NSC survival and early differentiation seen when NSC are transplanted alone. To address the challenges of cell damage during delivery and introduction into an injured and hostile microenvironment, we recently demonstrated that the co-encapsulation of NSC + EC in PEG microbeads promoted NSC quiescence prior to and post-delivery into a non-injury model, enabling NSC protection during delivery and escape from the microbeads only upon appropriate placement of the beads into the region of interest (Matta et al., 2019). In addition, PEG, known as an inert material, reduced inflammatory response compared to freely injected cells, suggesting these biomimetic units can be used to promote NSC survival, maintain NSC quiescence prior to injection and reduce inflammation that can inhibit NSC survival upon transplantation (Matta et al., 2019).

In the current study, we inject cell-encapsulated microbeads to an ICH cavity, rather than a non-injury model, to further validate the efficacy of our delivery system to another injury model. Here, we demonstrate that following 7 days of hemorrhage induction, the cavity was activated enough to degrade our MMP-degradable microbeads and allow for cell escape. Using a Brefeldin-A injection to allow for intracellular cytokine visualization, our results show that NSC + EC encapsulated microbeads lead to a more prominent VEGF-C secretion in the ICH cavity and tissue surrounding the cavity as compared to NSC encapsulated alone or microbeads with no cells. This provides further evidence that VEGF-C is produced by a co-culture of NSC + EC in response to injury as compared to NSC, agreeing with out in vitro findings. It has been demonstrated that stereotaxic injection of VEGF-C to the rodent brain resulted in an increase in the number of proliferation neural cells, suggesting VEGF-C can increase neurogenesis. Therefore, the co-delivery of NSC + EC may promote NSC survival and proliferation by providing greater access to secreted VEGF-C.

In summary, we have demonstrated that VEGF-C/VEGFR3 could promote NSC survival in a milieu with compromised nutrient availability such as an injured brain. To our advantage, EC secrete elevated levels of VEGF-C, and NSC VEGFR3 was elevated in response to cell contact with EC and in the presence of VEGF-C. There are other pro-survival factors which can also aid this response, many of which have been attributed to enhanced NSC survival.

These include insulin-growth factor-1 (IGF-1) and BDNF, which have demonstrated promising results as acute therapies. These have been administered effectively after 30 and 15 min post MCAO, respectively, and the growth factors led to a reduction in infarct volume (Greenberg and Jin 2006). In addition, a metabolic switch may play a role in allowing NSC to proliferate in an injury-state. It has been demonstrated that NSC survive with lactate in a glucose-free environment (Wohnsland et al., 2010). Interestingly, EC secrete lactate during ischemia (Zhang et al., 2020), so there may be a potential link between EC promoting a metabolic switch for NSC under GD that promotes survival. Nonetheless, the effect of VEGF-C was pronounced on NSC proliferation, reduction of cytotoxicity, and enhancement of NSC VEGFR3 expression. Future studies will be needed to determine the effects of NSC and EC co-transplantation on NSC differentiation, neurogenesis, and functional recovery in the rodent model. In total, the findings suggest that EC-derived VEGF-C aids in NSC survival and proliferation within injured tissue and should be investigated further as potential therapeutic to augment local stem cell therapies.

Supplementary Material

Refer to Web version on PubMed Central for supplementary material.

Acknowledgments

The authors acknowledge Hannah Beatty for her assistance and input for immunostaining reagents and protocols. The study was supported by NIH (R01EB016629-03).

Abbreviations:

BDNF	Brain-derived neurotrophic factor
CM	Conditioned media
EC	Endothelial cell
GD	Glucose deprivation
ICH	Intracerebral hemorrhage
NSC	Neural stem cell
OGD	Oxygen glucose deprivation
PBS	Phosphate Buffered Saline
PC	Pericyte
PEG	Polyethylene glycol
PEGDA	Polyethylene glycol diaciylate
SVZ	Subventricular zone
VEGF	Vascular endothelial growth factor

VEGFR3 Vascular endothelial growth factor receptor 3.

References

Alam A, Blanc I, Gueguen-Dorbes G, Duclos O, Bonnin J, Barron P, Laplace M-C, Morin G, Gaujarengues F, Dol F, Hérault J-P, Schaeffer P, Savi P, Bono F, 2012. SAR131675, a Potent and Selective VEGFR-3–TK inhibitor with antilymphangiogenic, antitumoral, and antimetastatic activities. Mol. Cancer Therap. 11 (8), 1637–1649. [PubMed: 22584122]

Alvarez-Buylla A, García-Verdugo JM, 2002. Neurogenesis in adult subventricular zone. J. Neurosci. 22 (3), 629–634. [PubMed: 11826091]

Askenase M, Sansing L, 2016. Stages of the inflammatory response in pathology and tissue repair after intracerebral hemorrhage. Semin. Neurol. 36 (03), 288–297. [PubMed: 27214704]

Azevedo PO, Lousado L, Paiva AE, Andreotti JP, Santos GSP, Sena IFG, Prazeres P, Filev R, Mintz A, Birbrair A, 2017. Endothelial cells maintain neural stem cells quiescent in their niche. Neuroscience 363, 62–65. [PubMed: 28893649]

Blanc I, Alam A, Duclos O, Gueguen G, Bonnin J, Laplace MC, Barron P, Dol F, Schaeffer P, Savi P, Bono F, 2010. SAR131675, a new potent selective VEGFR-3-TK inhibitor: effect on lymphangiogenic, tumor growth, and metastasis. J. Clin. Oncol. 28 (15_suppl) e13623–e13623.

Bressan RB, Dewari PS, Kalantzaki M, Gangoso E, Matjusaitis M, Garcia-Diaz C, Blin C, Grant V, Bulstrode H, Gogolok S, Skarnes WC, Pollard SM, 2017. Efficient CRISPR/Cas9-assisted gene targeting enables rapid and precise genetic manipulation of mammalian neural stem cells. Development 144 (4), 635–648. [PubMed: 28096221]

Calvo C-F, Fontaine RH, Soueid J, Tammela T, Makinen T, Alfaro-Cervello C, Bonnaud F, Miguez A, Benhaim L, Xu Y, Barallobre M-J, Moutkine I, Lyytikka J, Tatlisumak T, Pytowski B, Zalc B, Richardson W, Kessaris N, Garcia-Verdugo JM, Alitalo K, Eichmann A, Thomas J-L, 2011. Vascular endothelial growth factor receptor 3 directly regulates murine neurogenesis. Genes Dev. 25 (8), 831–844. [PubMed: 21498572]

Carmichael ST, 2006. Cellular and molecular mechanisms of neural repair after stroke: making waves. Ann. Neurol. 59 (5), 735–742. [PubMed: 16634041]

Chiu D, Peterson L, Elkind MSV, Rosand J, Gerber LM, Silverstein MD, 2010. Comparison of outcomes after intracerebral hemorrhage and ischemic stroke. J. Stroke Cerebrovasc. Dis. 19 (3), 225–229. [PubMed: 20434051]

Espagnolle N, Barron P, Mandron M, Blanc I, Bonnin J, Agnel M, Kerbelec E, Herault JP, Savi P, Bono F, Alam A, 2014. Specific inhibition of the VEGFR-3 tyrosine kinase by SAR131675 reduces peripheral and tumor associated immunosuppressive myeloid cells. Cancers 6 (1), 472–490. [PubMed: 24589997]

Flaherty ML, Haverbusch M, Sekar P, Kissela B, Kleindorfer D, Moomaw CJ, Sauerbeck L, Schneider A, Broderick JP, Woo D, 2006. Long-term mortality after intracerebral hemorrhage. Neurology 66 (8), 1182–1186. [PubMed: 16636234]

Foster B, Prussin C, Liu F, Whitmire JK, Whitton JL, 2007. Detection of intracellular cytokines by flow cytometry. Curr. Protoc. Immunol. Chapter 6: Unit 6 24.

Gao L, Xu W, Li T, Chen J, Shao A, Yan F, Chen G, 2018. Stem cell therapy: a promising therapeutic method for intracerebral hemorrhage. Cell Transplant. 27 (12), 1809–1824. [PubMed: 29871521]

Ghuman H, Matta R, Tompkins A, Nitzsche F, Badylak SF, Gonzalez AL, Modo M, 2020. ECM hydrogel improves the delivery of PEG microsphere-encapsulated neural stem cells and endothelial cells into tissue cavities caused by stroke. Brain Res. Bull.

Girouard H, Iadecola C, 2006. Neurovascular coupling in the normal brain and in hypertension, stroke, and Alzheimer disease. J. Appl. Physiol. 100 (1), 328–335. [PubMed: 16357086]

Gonzalez AL, Gobin AS, West JL, McIntire LV, Smith CW, 2004. Integrin interactions with immobilized peptides in polyethylene glycol diacrylate hydrogels. Tissue Eng. 10 (11–12), 1775–1786. [PubMed: 15684686]

Greenberg DA, Jin K, 2006. Growth factors and stroke. NeuroRX 3 (4), 458–465. [PubMed: 17012059]

Han J, Calvo C-F, Kang Tae H., Baker Kasey L., Park J-H, Parras C, Levittas M, Birba U, Pibouin-Fragner L, Fragner P, Bilguvar K, Duman Ronald S., Nurmi H, Alitalo K, Eichmann Anne C. and Thomas J-L (2015). "Vascular Endothelial Growth Factor Receptor 3 Controls Neural Stem Cell Activation in Mice and Humans." Cell Reports 10(7): 1158–1172. [PubMed: 25704818]

Hicks AU, Lappalainen RS, Narkilahti S, Suuronen R, Corbett D, Sivenius J, Hovatta O, Jolkkonen J, 2009. Transplantation of human embryonic stem cell-derived neural precursor cells and enriched environment after cortical stroke in rats: cell survival and functional recovery. Eur. J. Neurosci. 29 (3), 562–574. [PubMed: 19175403]

Jin K, Zhu Y, Sun Y, Mao XO, Xie L, Greenberg DA, 2002. Vascular endothelial growth factor (VEGF) stimulates neurogenesis in vitro and in vivo. Proc. Natl. Acad. Sci. U.S.A. 99 (18), 11946–11950. [PubMed: 12181492]

Lampe KJ, Heilshorn SC, 2012. Building stem cell niches from the molecule up through engineered peptide materials. Neurosci. Lett. 519 (2), 138–146. [PubMed: 22322073]

Lauridsen HM, Walker BJ, Gonzalez AL, 2014. Chemically- and mechanically-tunable porated polyethylene glycol gels for leukocyte integrin independent and dependent chemotaxis. Technology 02 (02), 133–143.

Le Bras B, Barallobre M-J, Homman-Ludiye J, Ny A, Wyns S, Tammela T, Haiko P, Karkkainen MJ, Yuan L, Muriel M-P, Chatzopoulou E, Bréant C, Zalc B, Carmeliet P, Alitalo K, Eichmann A, Thomas J.-Léon., 2006. VEGF-C is a trophic factor for neural progenitors in the vertebrate embryonic brain. Nat. Neurosci. 9 (3), 340–348. [PubMed: 16462734]

Lee S-H, Moon JJ, Miller JS, West JL, 2007. Poly(ethylene glycol) hydrogels conjugated with a collagenase-sensitive fluorogenic substrate to visualize collagenase activity during three-dimensional cell migration. Biomaterials 28 (20), 3163–3170. [PubMed: 17395258]

Lin R, Cai J, Nathan C, Wei X, Schleidt S, Rosenwasser R, Iacovitti L, 2015. Neurogenesis is enhanced by stroke in multiple new stem cell niches along the ventricular system at sites of high BBB permeability. Neurobiol. Dis. 74, 229–239. [PubMed: 25484283]

Lindvall O, Kokaia Z, 2010. Stem cells in human neurodegenerative disorders — time for clinical translation? J. Clin. Investig. 120 (1), 29–40. [PubMed: 20051634]

Marlier Q, Verteneuil S, Vandenbosch R, Malgrange B, 2015. Mechanisms and functional significance of stroke-induced neurogenesis. Front. Neurosci. 9, 458. [PubMed: 26696816]

Matta R, Lee S, Genet N, Hirschi KK, Thomas J-L, Gonzalez AL, 2019. Minimally invasive delivery of microbeads with encapsulated, viable and quiescent neural stem cells to the adult subventricular zone. Sci. Rep. 9 (1), 17798. [PubMed: 31780709]

Mozaffarian D, Benjamin EJ, Go AS, Arnett DK, Blaha MJ, Cushman M, Das SR, Ferranti S.d., Després J-P, Fullerton HJ, Howard VJ, Huffman MD, Isasi CR, Jiménez MC, Judd SE, Kissela BM, Lichtman JH, Lisabeth LD, Liu S, Mackey RH, Magid DJ, McGuire DK, Mohler ER, Moy CS, Muntner P, Mussolino ME, Nasir K, Neumar RW, Nichol G, Palaniappan L, Pandey DK, Reeves MJ, Rodriguez CJ, Rosamond W, Sorlie PD, Stein J, Towfighi A, Turan TN, Virani SS, Woo D, Yeh RW, Turner MB, 2016. Executive summary: heart disease and stroke statistics—2016 update. Circulation 133 (4), 447–454. [PubMed: 26811276]

Nakagomi N, Nakagomi T, Kubo S, Nakano-Doi A, Saino O, Takata M, Yoshikawa H, Stern DM, Matsuyama T, Taguchi A, 2009. Endothelial cells support survival, proliferation, and neuronal differentiation of transplanted adult ischemia-induced neural stem/progenitor cells after cerebral infarction. Stem Cells 27 (9), 2185–2195. [PubMed: 19557831]

Ottone C, Parrinello S, 2015. Multifaceted control of adult SVZ neurogenesis by the vascular niche. Cell Cycle 14 (14), 2222–2225. [PubMed: 26115376]

Park KI, Teng YD, Snyder EY, 2002. The injured brain interacts reciprocally with neural stem cells supported by scaffolds to reconstitute lost tissue. Nat. Biotechnol. 20 (11), 1111–1117. [PubMed: 12379868]

Pollard SM, Conti L, Sun Y, Goffredo D, Smith A, 2006. Adherent neural stem (NS) cells from fetal and adult forebrain. Cereb. Cortex 16 (Suppl 1), i112–i120. [PubMed: 16766697]

Ruan L, Wang B, ZhuGe Q, Jin K, 2015. Coupling of neurogenesis and angiogenesis after ischemic stroke. Brain Res. 1623, 166–173. [PubMed: 25736182]

Sacco S, Marini C, Toni D, Olivieri L, Carolei A, 2009. Incidence and 10-year survival of intracerebral hemorrhage in a population-based registry. Stroke 40 (2), 394–399. [PubMed: 19038914]

Shin Y-J, Riew T-R, Park J-H, Pak H-J, Lee M-Y, 2015. Expression of Vascular Endothelial Growth Factor-C (VEGF-C) and Its Receptor (VEGFR-3) in the Glial Reaction Elicited by human mesenchymal stem cell engraftment in the normal rat brain. J. Histochem. Cytochem. 63 (3), 170–180. [PubMed: 25473093]

Singh G, Siddiqui MA, Khanna VK, Kashyap MP, Yadav S, Gupta YK, Pant KK, Pant AB, 2009. Oxygen glucose deprivation model of cerebral stroke in PC-12 cells: glucose as a limiting factor. Toxicol. Mech. Methods 19 (2), 154–160. [PubMed: 19778261]

Smith EJ, Stroemer RP, Gorenkova N, Nakajima M, Crum WR, Tang E, Stevanato L, Sinden JD, Modo M, 2012. Implantation site and lesion topology determine efficacy of a human neural stem cell line in a rat model of chronic stroke. Stem Cells 30 (4), 785–796. [PubMed: 22213183]

Sukumari-Ramesh S, Alleyne CH, Dhandapani KM, 2012. Astrogliosis: a target for intervention in intracerebral hemorrhage? Transl. Stroke Res. 3 (S1), 80–87. [PubMed: 24323864]

Taylor RA, Chang C-F, Goods BA, Hammond MD, Mac Grory B, Ai Y, Steinschneider AF, Renfroe SC, Askenase MH, McCullough LD, Kasner SE, Mullen MT, Hafler DA, Love JC and Sansing LH (2017). “TGF-β1 modulates microglial phenotype and promotes recovery after intracerebral hemorrhage.” The Journal of Clinical Investigation 127(1): 280–292. [PubMed: 27893460]

Taylor RA, Sansing LH, 2013. Microglial responses after ischemic stroke and intracerebral hemorrhage. Clin. Dev. Immunol. 2013, 746068. [PubMed: 24223607]

Wohnsland S, Bürgers HF, Kuschinsky W, Maurer MH, 2010. Neurons and neuronal stem cells survive in glucose-free lactate and in high glucose cell culture medium during normoxia and anoxia. Neurochem. Res. 35 (10), 1635–1642. [PubMed: 20602256]

Xiong Y.-jie., Yin B, Xiao L.-chen., Wang Q, Gan L, Zhang Y.-chi., Zhang S.-ming., 2013. Proliferation and differentiation of neural stem cells co-cultured with cerebral microvascular endothelial cells after oxygen-glucose deprivation. J. Huazhong Univ. Sci. Technol. [Medical Sci.] 33 (1), 63–68.

Zarkada G, Heinolainen K, Makinen T, Kubota Y and Alitalo K (2015). “VEGFR3 does not sustain retinal angiogenesis without VEGFR2.” Proceedings of the National Academy of Sciences 112(3): 761–766.

Zhang RL, Chopp M, Roberts C, Liu X, Wei M, Nejad-Davarani SP, Wang X, Zhang ZG, 2014b. Stroke increases neural stem cells and angiogenesis in the neurogenic niche of the adult mouse. PLoS One 9 (12), e113972. [PubMed: 25437857]

Zhang RL, Chopp M, Roberts C, Liu X, Wei M, Nejad-Davarani SP, Wang X and Zhang ZG (2014). “Stroke increases neural stem cells and angiogenesis in the neurogenic niche of the adult mouse.” PloS one 9(12): e113972–e113972. [PubMed: 25437857]

Zhang J, Muri J, Fitzgerald G, Gorski T, Gianni-Barrera R, Masschelein E, D’Hulst G, Gilardoni P, Turiel G, Fan Z, Wang T, Planque M, Carmeliet P, Pellerin L, Wolfrum C, Fendt S-M, Banfi A, Stockmann C, Soro-Arnáiz I, Kopf M, De Bock, K, 2020. Endothelial lactate controls muscle regeneration from ischemia by inducing Mlike macrophage polarization. Cell Metab. 31(6), 1136–1153.e1137. [PubMed: 32492393]

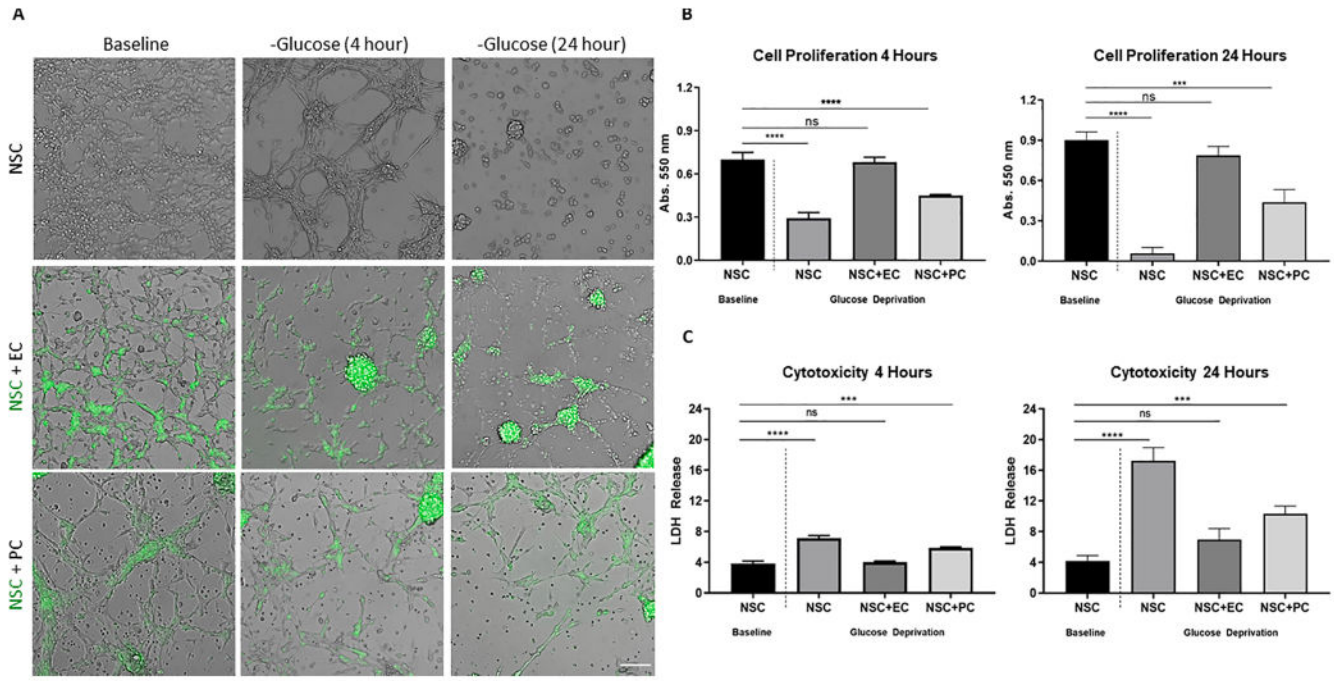

Fig. 1.

EC increase NSC proliferation and decrease NSC cytotoxicity during glucose deprivation. A) NSC, NSC + EC, and NSC + PC at baseline (left column), 4 h of glucose deprivation (middle column) and 24 h of glucose deprivation (right column), using NSC with a GFP tag in co-cultures. Scale bar (100 μm representative of all images. B) Cell proliferation for NSC baseline control and NSC, NSC + EC, and NSC + PC under GD at 4 h (left) and 24 h (right). C) Cell cytotoxicity for NSC baseline control and NSC, NSC + EC, and NSC + PC under GD at 4 h (left) and 24 h (right). Data are represented as mean ± SEM; n = 3.

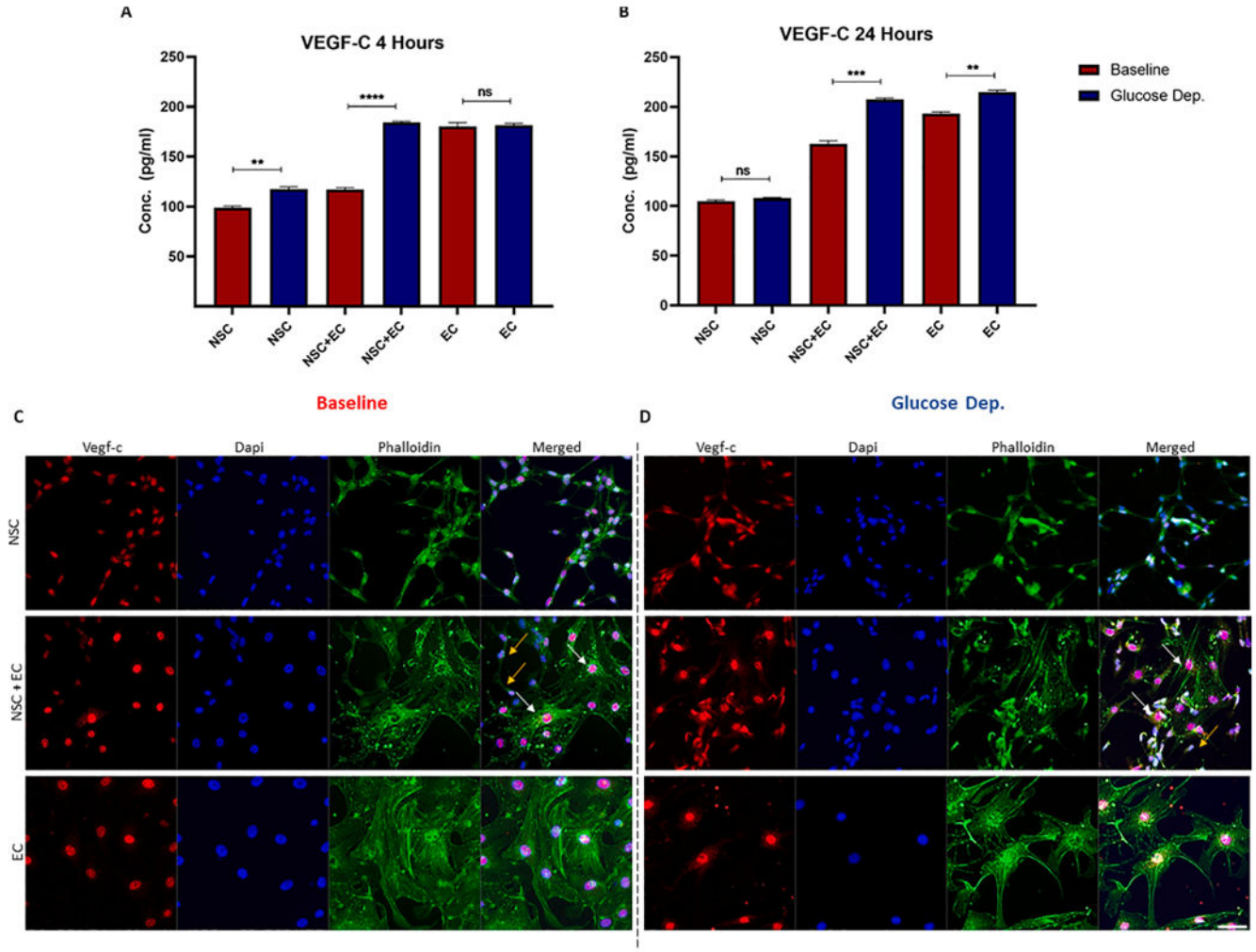

Fig. 2.

VEGF-C secretion is increased in co-cultures of NSC + EC during glucose deprivation. A) VEGF-C secreted levels for NSC, NSC + EC, and EC at 4 h under baseline and GD and B) at 24 h under baseline and GD. C) Immunofluorescent images for NSC, NSC + EC, and EC at 4 h under C) baseline and D) GD, staining against VEGF-C (red), Dapi (blue), and Phalloidin (green). Scale bar (50 μm) representative of all images. Data are represented as mean ± SEM; n = 3.

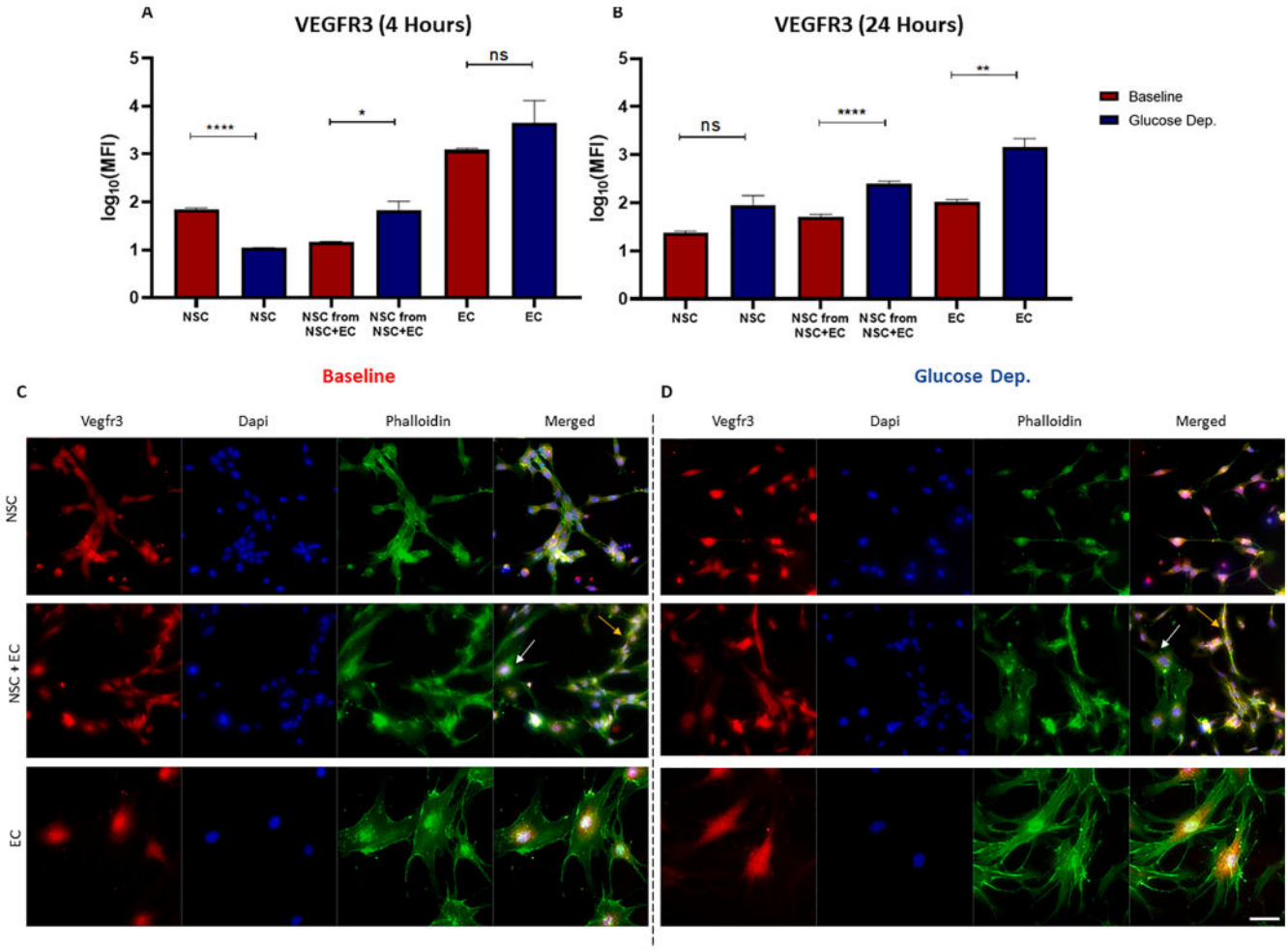

Fig. 3.

VEGFR3 expression is increased in co-cultures of NSC + EC during glucose deprivation. A) VEGFR3 expression for NSC, NSC from NSC + EC, and EC at 4 h under baseline and GD and B) at 24 h under baseline and GD. C) Immunofluorescent images for NSC, NSC + EC, and EC at 4 h under C) baseline and D) GD, staining against VEGFR3 (red), Dapi (blue), and Phalloidin (green). Scale bar (50 μm) representative of all images. Data are represented as mean ± SEM; n = 3.

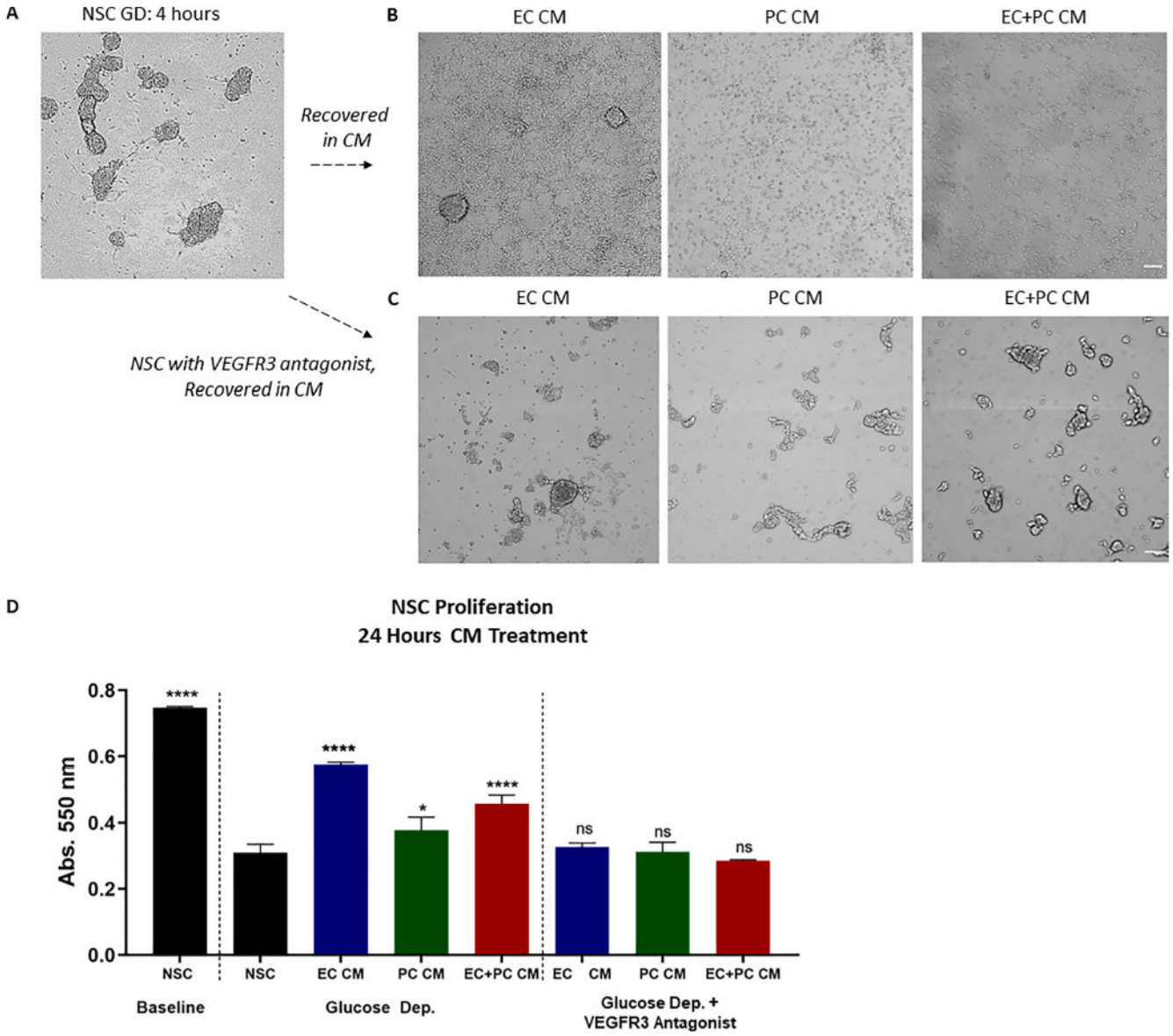

Fig. 4.

EC conditioned media (CM) increases NSC proliferation following glucose deprivation with VEGFR3 antagonist. A) NSC under 4 h of GD, B) recovered in EC, PC, and EC + PC CM. C) NSC with VEGFR3 antagonist SAR131675, at a concentration of 50 nM for 24 h, recovered in EC, PC, and EC + PC CM. D) NSC proliferation for baseline control and GD, NSC recovered in EC, PC, and EC + PC CM, and NSC with VEGFR3 antagonist recovered in EC, PC, and EC + PC CM. Scale bar (100 μm) representative of all images. Data are represented as mean ± SEM; n = 3.

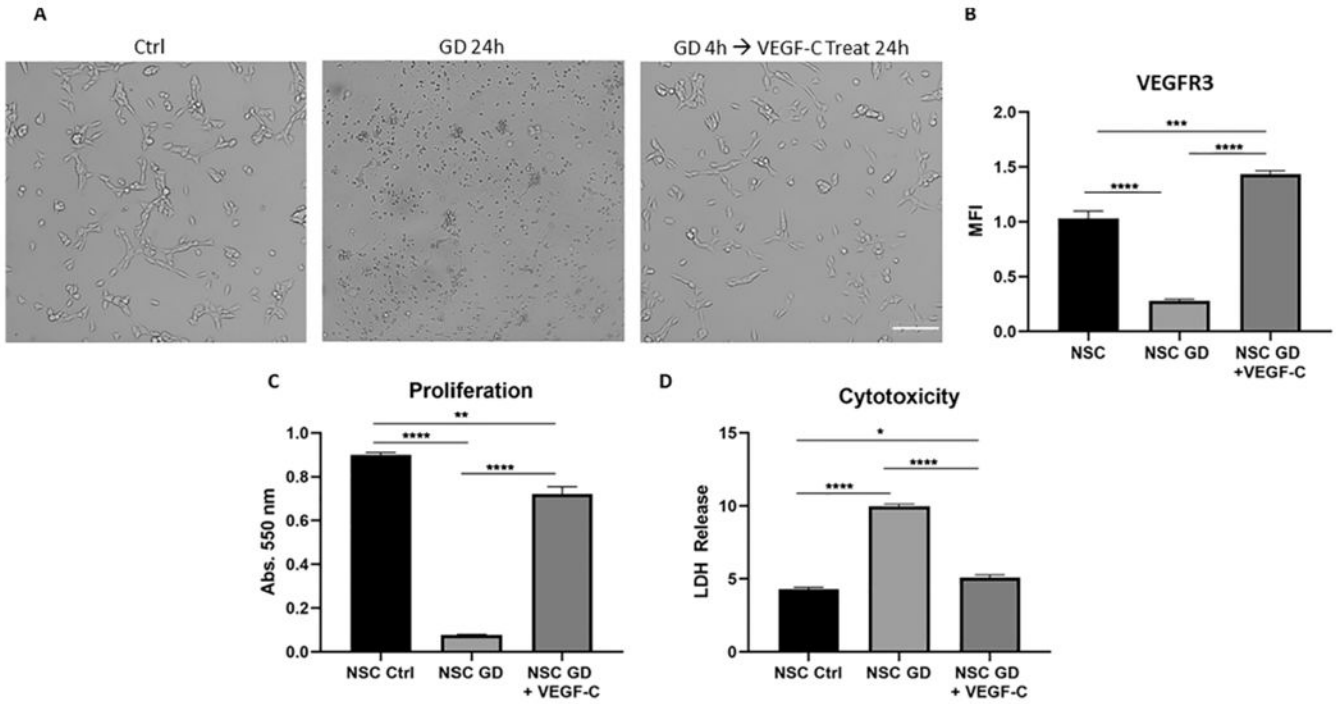

Fig. 5.

Exogenous treatment with VEGF-C increases VEGFR3 expression, promotes NSC proliferation, and decreases cytotoxicity. A) Brightfield images of NSC control, NSC under GD for 24 h, and NSC under GD for 4 h then treated with VEGF-C at a concentration of 10 ng/ml for 24 h. B) VEGFR3 quantification, C) NSC proliferation, and D) NSC cytotoxicity for NSC control, NSC under GD for 24 h, and NSC under GD for 4 h then treated with VEGF-C for 24 h. Scale bar (100 μm) representative of all images. Data are represented as mean ± SEM; n = 3.

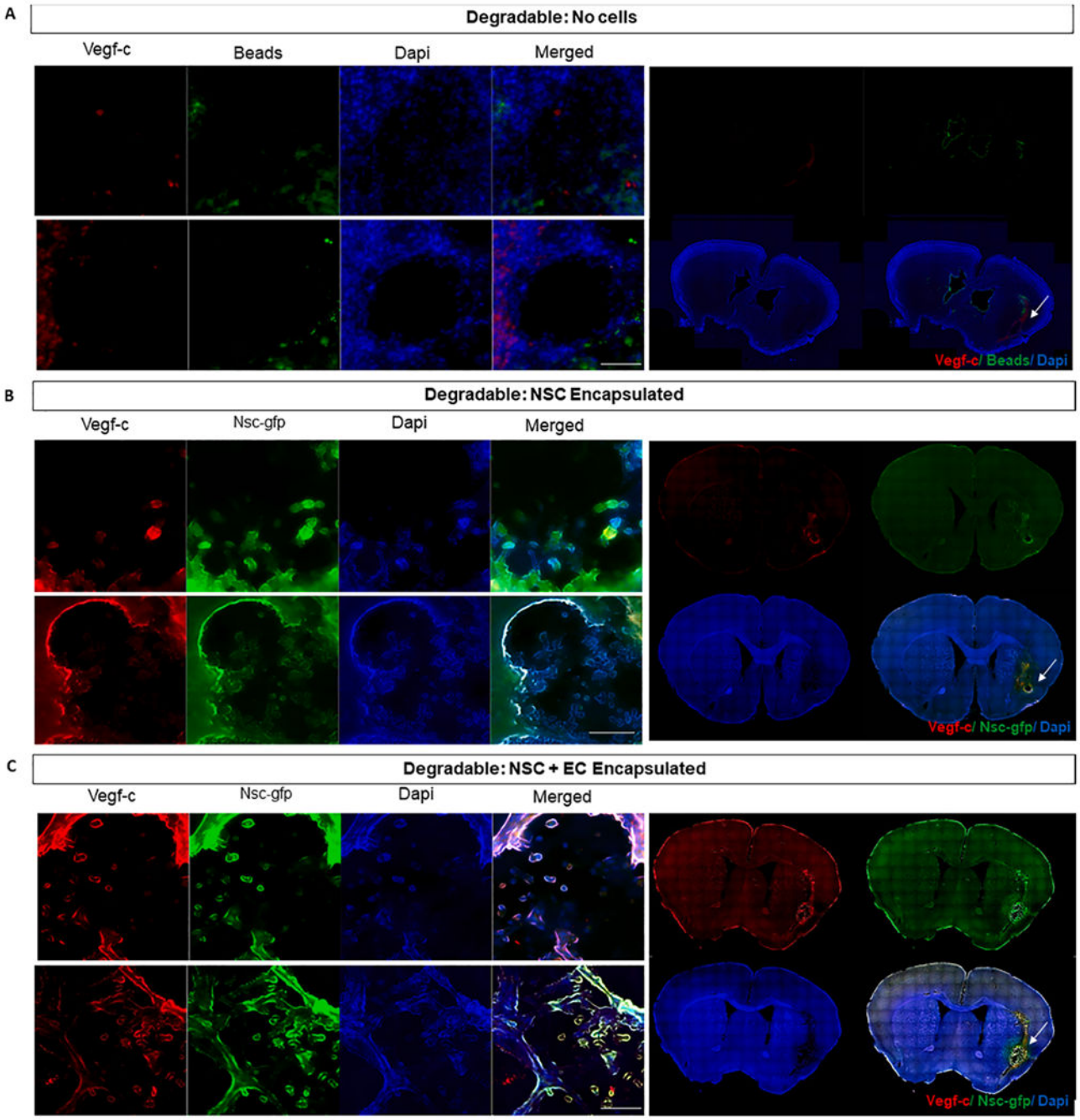

Fig. 6.

NSC + EC encapsulated microbeads led to VEGF-C secretion in tissue A) ICH brain sections with implanted degradable green microbeads containing no cells, staining against VEGF-C (red), microbeads (green), and Dapi (blue). B) ICH brain sections with implanted degradable microbeads containing encapsulated NSC-GFP and C) co-encapsulated NSC-GFP and EC, staining against VEGF-C (red), NSC-GFP (green), and Dapi (blue). Scale bar (50 μm) representative of all images. N = 2–3 per condition.